The Influence of Tool Tilt Angle on the Friction Stir Welding Characteristics of Wrought Magnesium Alloy Plates

Anil Kumar Deepati*

Department of Mechanical Engineering Technology, CAIT, Jazan University, Jizan 82817-2820, Kingdom of Saudi Arabia

*Corresponding author: Tel: +966 173295000 (Extn. 3074); +966 500648537

*Corresponding author e-mail: adeepati@jazanu.edu.sa ; flytoanil@gmail.com

Abstract

During the friction stir welding (FSW) process, the influence of the tool tilt angle (TA) over mechanical characteristics and microstructure of wrought magnesium alloy was examined. FSW was performed using fixtures and a clamping system specially developed for the present work, by varying the TA from 0^o-3^o with an interval of 1^o whilst the tool rotational and traverse speed were stable at 1400rpm and 112mm/min, distinctively. Microstructural characterization, hardness measurement, and tensile testing were executed to evaluate the FSW joint characteristics. When compared to other joints, an experimental analysis showed that the joint produced at 0^o TA has better mechanical and metallurgical properties. The incorporated parameters 1400tool rpm, 112mm/min traversing speed produced defect-free welds and improved joint strength with the utmost tensile strength of 187MPa and micro-hardness of 75HV. Tensile strength decreased with increasing tool tilt angle, with the lowest joint strength of 161 MPa recorded at the maximum TA 3^o. The coarse grains of the original alloy ~35 m altered to refined grains at the weld stirred zone, with an average grain size of 11 μm, 14 μm, 16 μm, and 18 μm, corresponding to 0^o, 1^o, 2^o, and 3^o TAs, respectively.

Keywords: Friction stir welding (FSW), Tool Tilt angle (TA), AZ31B, Tool traversing speed, Microstructure, Mechanical Properties, Tensile strength.

1. Introduction

FSW is an efficacious technique to weld metals in solid state conditions and this process is considered to be the most appropriate method to weld lower melting point metals and dissimilar alloys which are difficult to weld using standard fusion welding methods. [1,2]

FSW is performed with a revolving cylindrical tool equipped with a pin of diameter lesser than the shoulder size. The tool pin is inserted between two plates until the shoulder reaches the workpiece's top surface [3]. The rotating tool remains in the same place after plunging to achieve the sufficient temperature required for welding is called the dwell time. This could be approximately form 5-10 seconds then the tool traverses along the weld line to complete the welding. Figure. 1 depicts the FSW basic principle and parts of the FSW tool.

Figure 1.

Friction stir weld joint types and properties are reported by Nandan et al., [4] During the movement of the tool laterally on the middle of the weld joint, heat caused by friction generates amongst the rotating tool to the workpiece leading to plasticizing or softening the material and then mechanically mixing the softened material, subsequently the joining happens from the trailing side as the tool moves forward. Friction stir welding is suitable to weld alloys such as aluminum, copper, titanium, mild steel, stainless steel, and magnesium; in addition to that it can also weld polymers as well [5]. Alternative fusion welding procedures, such as tungsten inert gas welding and electron beam welding, are impractical for joining lower melting temperature metals such as aluminum alloy and magnesium alloy [6,7]. FSW is performed using a non-consumable tool, hence, the weld joints are generally free from defects like solidification cracking, liquation cracking, and porosity [8]. This process is widely implemented to fabricate lightweight materials for application in the rail, marine, automotive, and aerospace industries [3]. This process is also used to weld different types of joint configurations as illustrated in Figure. 2 [9].

Figure 2.

The microstructural development and temperature distribution during FSW are influenced by process factors for example the rotating speed of the tool, traverse speed of the tool, tilt angle, plunge depth, and shape of the tool pin. Some of the other process variables like axial force, tool offset, and material locations also influence the heat generation, microstructure, and mechanical properties of the weld joint. Some of the welding variables involved during the FSW process are depicted in the schematic diagram in Figure. 3. It is not straightforward to determine how welding speed, rotating speed, and heat input relate to one another. The rate of heat generation increase with increasing rotational speed and decreasing traverse speed. If the materials are not properly softened due to insufficient heat, different types of defects may occur in the weld zone. On the other hand, a welding temperature that is too high causes an unfavorable change in the material's microstructure and mechanical characteristics in the

weld zone. Generally, FSW is performed at a slightly lean or tilted position because the downward applied forces can affect the joint, so to prevent this condition a tilt is given. To guarantee that the essential downward force is delivered and that the tool thoroughly penetrates the weld, the plunge depth must be properly adjusted. Providing insufficient tool plunging results in low-quality weld owing to the inadequate plunging of the material while an excessive plunge depth leads to rubbing of the tool pin on the backing plates. As a result, to create a flawless and durable joint, appropriate welding parameters must be chosen.

The tool tilt angle plays an important role in achieving high-quality FSW joint properties. Mehta and Badhek [10] examined the impact of tilt angle (TA) over the characteristics of dissimilar FSW joints of copper to aluminum by varying the TA's from 0^o to 4^o with 1^o intervals while holding all other parameters constant. The greatest tensile properties were attained at a TA of 4 degrees. Anil Kumar et al., [9] examined the consequence of right-hand and left-hand threads on pin geometry and the bigger shoulder size of the FSW tool on the joint characteristics of dissimilar welds of Al-Cu neglecting the tool tilt angle. Tensile testing and Microhardness measurements were used to assess the mechanical properties of joints. The microstructure of the joints was studied using optical microscopy, SEM, and EDX spectroscopy.

Suryakanta Sahu et al.,[11] friction stir welded for a dissimilar metal combination of Magnesium to DP steel and studied the influence of tool rotation speed and traverse speed on the join properties. They fabricated the FSW joints using tool RPMs of 800 and 1600 and traverse speeds of 50, 100, and 150 mm/min, respectively by keeping tool plunge depth, and tool tilt angle of 0.2mm, 2° was kept constant during the welding. EDS and X-ray studies were also performed to understand the microstructural changes. They discovered that concerning AZ31B, the highest joint efficiency of 76.4% was attained.

Elyasi et al. [12] evaluated the effects of TA on FSW joints of AA1100 to A441 AISI butt configuration using TAs of 1^o, $2^{o,}$ and 3^o. The findings revealed that as the TA grew, so did the correlation of the two metals as well as the axial force of the tool. More surfaces mingled, internal mixing occurred, and frictional heat was generated as tool TA increased. Muhayat et al. [13] investigated how tilt angle and plunge depth affected the tensile performance of AA5083-H116 FSW joints. Mechanical testing results exhibited higher joint strength with increasing plunge depth and inclination angle. Shah and Badheka [14] used aluminum alloy

7075-T651 as the parent metal in an FSW experiment to investigate the impact of TA on joint microstructures, tensile behavior by altering the TA from 0^o-6^o. The weld made with 2^o TA yielded joints without defects with exceptional microstructures and mechanical properties. Meshram and Reddy [15] attempted to inspect the influence of tilt angle on defect formation by changing tool TA from 0^o-3^o with maintaining a gap of 0.5^o. Authors reported that the welds created with 1^o-2^o tilt angle produced defect-free joints owing to proper material mixing. Numerous researchers [16-18] conducted FSW studies to explore the influence of tool TA on the metallographic and mechanical qualities of welds

Figure 3.

Zia-wei et al.,[19] investigated the joint properties of 1.8mm thick AZ31 magnesium all using probe-less shoulder tools with no tilt angle, and produced acceptable welds with a shear strength of 4.22kN at tool speed of 1180 rpm. Asadi parviz and Mohammad Hosein Mirzaei et al., [20, 21] studied the effect of tool pin profile on material flow using a double shoulder tool on magnesium alloy. They co-related the material flow patterns, temperature, and strain distribution obtained on welds using a double shoulder FSW tool by simulation analysis.

Cojocaru et al., [22] compared the welds of A31B magnesium alloys in a traditional FSW process and an inert gas-assisted FSW process. They identified the welds produced under an inert gas environment exhibit greater mechanical properties compared to the classic FSW method. Creep behavior studies on various FSW weld zones are also performed on magnesium alloys [23]. Anil Kumar et al., [24] examined the consequence of right-hand and left-hand threads on pin geometry and the bigger shoulder size of the FSW tool on the joint characteristics of dissimilar welds of Al-Cu neglecting the tool tilt angle. Tensile testing and Microhardness measurements were used to assess the mechanical properties of joints. The microstructure of the joints was studied using optical microscopy, SEM, and EDX spectroscopy. Additionally, some researchers reported the joint characteristics, and material flow of dissimilar alloys joined by FSW for magnesium to aluminum, magnesium to magnesium alloys, and magnesium to ferrous alloys [25-28].

Few recent investigations were reported on parametric optimization of FSW of aluminum alloys by Taguchi-based analysis focused on the effect of tilt angle on joint strength and electrical conductivity [29-31]. The influence of tool tilt angle on the FSW of magnesium alloys is reported less comparatively FSW of aluminum alloys. The effect of the tilt angle of double-sided FSW was reported by Ankit Thakur et al.[32]. They compared the 0^0 and 2^0 tilt

angles using scrolled shoulder and screwed pin profiles and reported 74%, and 87% joint efficiencies by double-sided FSW. Liangwen Xie et al.,[33] identified a B-fiber texture on the weld centerline and under shoulder surface on welding of Mg–4.6Al–1.2Sn–0.7Zn magnesium alloy. The texture intensity pattern along the weld zone was investigated using an electron backscatter diffraction method. Further, they studied the joint properties of magnesium alloys using three types of threaded pin profiles. The increase in the depth of thread from 0 to 0.75 causes adequate material flow and grain refinement in the weld zone [34].

Fernanda RC. et al.,[35] welded a but joint of 2mm thick of AZ31 magnesium alloy by varying the gap widths between weld plates and noticed that increasing the gap between the weld plated the thickness of the weld zone reducing. The ultimate tensile strength of the welds and the fracture strain are not affected by the variations in the gap width. Zhe Liu et al.,[36] investigated the joint performance concerning process parameters evaluated by refill friction stir spot welding of magnesium alloys. Grain refinement and tensile strength improvement were observed at 1500 tool rpm with a 1.4mm plunge depth. Unnikrishnan et al.,[37] reviewed a detailed report of post-welding material properties, microstructure, and wear mechanism pattern reported on FSW of magnesium alloys with automotive applications. With the application of low welding temperature, the welds produced by FSW possess superior joint strength. Improvement in strength, hardness, ductile nature, and oxide resistance increases interest in magnesium alloys for transportation and structural applications.

The Magnesium alloy is been used in many other engineering applications where light weight is considered a significant factor. Although FSW is one of the best ways to join magnesium and its alloys. From the published literature it is evident that the majority of the researchers focussed on the tool rpm and tool traverse speeds on the FSW of magnesium alloys, but the effect of tool tilt angle has been ignored. The current study intends to analyze the effect of variation in the FSW tool tilt angle on the microstructure and mechanical properties of AZ31B Mg alloy. The experimental investigation was performed on a vertical axis semi-automated milling machine utilizing a designed FSW setup in this study. The base material was AZ31B Mg alloy, and the influence of TA on joint characteristics was investigated using metallographic analysis and mechanical testing.

2. Experimental Procedure

In the butt joint arrangement, wrought magnesium alloy with plate dimensions of 110 x 50 x 3 mm was friction stir welded. Before welding, the edges of the specimens were honed on a surface grinding machine and cleaned with acetone. The chemical composition and mechanical properties of the parent materials are shown in Tables 1 and 2. The FSW experiments were performed using fixtures and a clamping system especially designed and developed for this work, as shown in Figure. 4. The width of the backing plates and fixtures can be increased depending on the size of the plates being welded, while the length was calculated based on the dimensions of the milling machine table that was available. It is frequently used for friction stir welding of aluminum alloys and is made of H13 steel. The tool pin is 2.8 mm in length and has a 16 mm shoulder size with a concave surface of 4° angle that tapers from 5mm to 3 mm. The welding involved varying the tool tilt angle while maintaining stable spindle rotation and traverse speed of 1400rpm and 112mm/min sequentially. The process parameters were chosen based on trial tests that took into account parameters from the literature as well as the machine's available spindle and welding speeds. All sets of the experiment underwent microstructural characterization and mechanical testing.

Figure. 4.

Table 1

Table 2

The welded samples were machined for tensile testing using Wire-cut EDM under ASTM E8 standards; the geometry and dimensions of the tensile test specimen are given in Figure. 5. The ultimate tensile strength (UTS) of FSW joints were determined utilizing tensile testing using a 100 kN universal testing equipment, INSTRON 8801, at a testing speed of 1 mm/min. Wire-cut EDM was used to cut the samples for metallographic examination into 34 x 12 x 3 mm pieces, which were then cleaned with acetone to eliminate contaminants. For 10 seconds, the samples were etched in a solution of 70 mL ethanol, 10 mL of both acetic acid and distilled water each, and 4.2 g picric acid. The microstructural study was carried out using optical microscopy (OM). The Vickers micro-hardness across the weld-center line of each sample was measured using a Vickers micro-hardness tester with an indentation period of 15 seconds and a load of 100 gf.

Figure. 5

3. Results and Discussion

Figure. 6 represents the welded plates of wrought magnesium alloy joined with different tool tilt angles ranging from 0^o-3^o. Through visual observation, the weld surface was inspected and it revealed a defect-free and smooth surface finish while the internal defect was examined by microscopic examination. All welded plates contain a thin flash but it does not have any influence on joint properties since it occurs just due to high heat generations and the application of major compressive force during the welding process. The flashes were removed manually before sectioning samples for microstructural analysis and mechanical testing to prevent unnecessary encumbrance. The visual inspection of the sample reveals that the sound welds produced both the top and bottom parts of the weld. Further investigation was carried out to analyze the joint properties.

Figure. 6**.**

Figure 7 depicts macrographs of FSW joints acquired at various tilt angles. Except for a joint welded with a 3^o tilt angle, which has an onion ring shape at the border amongst the TMAZ and the heat-affected zone(HAZ) on the welds, the forms of the stir zones of all welds are nearly identical. With a 0^o tilt angle, the metal connected to the tool shoulder moves in the same direction as the shoulder moves, taking into account the downward horizontal displacement of the metal all around the probe. In light of the tool's simultaneous rotational and translational movement, the tilt imparted to the FSW-tool consequences in forcing the metal down to the retreating side from the advancing side, and vice versa. Because of the tilt angle, this material descending at the back end of the tool shoulder can be regarded as a forging action. With a 0^o TA, the shoulder makes total contact with the plates, allowing more metal carried to the trailing part at the weld's upper surface.

Figure. 7.

3.1 Microstructural Characterization

To explore the impact of TA on the conditions of microstructure and tensile characteristics, the metallographic examination was done on joints manufactured with varied tool tilt angles. From the previous studies it has been observed that the FSW specimen is generally

categorized into 4 different zones [2]: (1) base metal zone (BMZ), it is also called unaffected zone; (2) heat affected zone (HAZ), an insignificant welding heat transfers into this zone, hence, the properties of metals do not change in this region; (3) thermo-mechanically affected zone (TMAZ), the materials in this zone experienced high welding temperature and the material tends to undergo deformation and; weld nugget zone or stir zone (SZ), the materials in this area deform plastically and grain structure completely changed as a result of stirring action of the tool pin. The weld microstructure of the parent material AZ31B Mg alloy is shown in Figure 8. Grain structures of HAZ and TMAZ of the FSW joint made with 0^o tilt angle are depicted in Figure 9. Whereas Figure 9(a) and 9(b) represents HAZ and TMAZ zones and are not similar. As illustrated in Fig. 8, the HAZ is located between the TMAZ and the PM, and it merely experiences a heat cycle with no plastic deformation. As a result, HAZ retains a microstructure similar to PM, with a slightly higher grain size. The grains at the TMAZ are elongated towards bottom right of the captured picture shown in Figure 9(b), the reason for this elongation is due to tool vertical plunge force and tool clockwise rotations.

Heat affected zone consists of elongated grains, and the average grain size of HAZ and TMAZ is ~28 μm and 20 μm, respectively. Stir zone microstructures of joints made at different tool TAs are shown in Figure 10(a)-Figure 10(d). TMAZ is located adjacent to SZ and is subjected to heat and stress from mechanical too forces[38, 39]. As a result, continual dynamic recrystallization (CDRX) develops in the zone, and small equiaxial grains nucleate at the grain boundaries of the parent grains and expand to some degree, resulting in a mixed zone of bulky and fine grains, as illustrated in Figure 10. Owing to dynamic recrystallization, the coarse grains of parent metal ~35 μm reformed into fine grains in the nugget or stir-zone with an average grain diameter of 11 μm, 14 μm, 16 μm and 18 μm corresponding to 0^o, 1^o, $2^{o,}$ and 3^o TAs, respectively. The joint made with a 0^o tilt angle showed finer grains when compared with joints created with other TAs, which contributed to higher tensile properties of a joint fabricated with this parameter.

Figure. 8.

Figure. 9.

Figure 10.

3.2 Mechanical Properties of FSW Joints

Figure 11 depicts the micro-hardness distribution curve of FSW joints manufactured at various tilt degrees. The weld nugget zone had the utmost hardness value of 75 HV at 0^o TA, while the thermo-mechanically impacted zone had the lowest hardness value of 52 HV at 3^o TA. It was discovered that when tool TAs increased from 0^o-3^o, the hardness values in SZ decreased. Micro-hardness was found to be higher in SZ than in the base material, but lower in TMAZ than in the parent metal. The hardness loss in TMAZ is attributed to precipitation coarsening, whereas the enhanced micro-hardness value in SZ is due to refined grain structure under the impact of tool pin stirring action. According to the published literature [40- 42], the tensile property distribution of FSW joints differs from that of micro-hardness, such as the stir zone(SZ) hardness is clearly higher than parent metal(PM) hardness; however, SZ tensile strength is just barely lower than PM tensile strength.

The distribution of micro-hardness asymmetry in Figure 11 is characteristic of FSW joints due to non-uniform heat distribution and material movement. To examine the hardness value, a trend line was plotted for each of the four joints, highlighting the variance in hardness value in each location.

Figure 11.

The photographs of tensile specimens before and after fracture are illustrated in Figure 12. The welds made with a tilt angle of 0^o-2^o broke at the border between the stir zone and the TMAZ on the advancing side(AS) while a joint made with 3^o fractured at the boundary between SZ and TMAZ on the retreating side (RS). It has been observed that the joint efficiency (JE) decreased with increasing tool TA and the highest JE of 76% of wrought magnesium alloy was achieved at 0^o TA. At maximum tool TA 3^o, the joint efficiency reaches the lowest value of 65% of the base alloy.

Figure 12

Figure 13 depicts the tensile characteristics of the joint at various tilt degrees. All TAs produced defect-free welds with good joint strength, having a maximum tensile strength of 187MPa, a yield strength of 138MPa, and a total elongation of 8%. The weld joint formed with TA of 3^o had the lowest joint characteristics of 160MPa UTS, 121MPa yield strength, and 6% total elongation, corresponding to the lowest micro-hardness values. Tensile properties i.e., maximum strength, yield strength, and elongation have all been found to decrease as the tilt angle increases.

Figure 13.

4. Conclusions

The effect of the tilting angle of the FSW tool on the FSW weld joint condition was evaluated by performing metallographic analysis and mechanical testing. From the investigation results, the following conclusions are made:

1. Elongated grains were seen in the heat-impacted zone, with the average grain size of the HAZ and TMAZ being 28μm and 20μm, respectively. The bigger grains of parent material 35 m transformed into fine grains in the stir zone due to dynamic recrystallization, with grain diameters of 11 μm, 14 μm, 16 μm, and 18 μm corresponding to 0^o, 1^o, 2^o, and 3^o tilt angles, respectively.
2. Maximum hardness values of 75 HV were observed in the stir zone at 0^o TA, while decreased hardness values of 52 HV were observed in a thermo-mechanically impacted zone at 3^o TA. SZ hardness rating drops as tool TAs increase from 0^o-3^o.
3. The joint efficiency decreased with increasing tool TA and the highest JE i.e. 76% of AZ31B Mg alloy was showed at 0^o TA. At maximum tool TA 3^o, the joint efficiency reaches the lowest value i.e. 65% of the base alloy.
4. Defect-free welds with a maximum strength of 187 MPa, yield strength of 138 MPa, and elongation of 8% were produced by all TAs. The weld joint obtained with a TA of 3^o indicated the lowest joint characteristics of 160 MPa UTS, 121 MPa yield strength, and 6% elongation, correlating to the lowest micro hardness values.

Conflict of Interest

The author declares that no real or potential conflicts of interest are there in this paper.

References

1. Zhenguo, G. Tiejun, Ma. Xiawei, Y. et al. "Multi-scale analyses of phase transformation mechanisms and hardness in linear friction welded Ti17(α+β)/Ti17(β) dissimilar titanium alloy joint", Chinese J. of Aer., 37(1) pp. 312-324 (2023). https://doi.org/10.1016/j.cja.2023.08.018.
2. Guo, Z.G. Ma, T.J. Yang, X.W. Tao, J. et al. "In-situ investigation on dislocation slip concentrated fracture mechanism of linear friction welded dissimilar Ti17(α+β)/Ti17(β) titanium alloy joint", Mat. Sci. and Engg., A, 872-144991 (2023). https://doi.org/10.1016/j.msea.2023.144991.
3. Thomas, W.M and Nicholas, E.D. "Friction stir welding for the transportation industries". *Mater.& Des.*, 18, pp. 269–273 (1997). https://doi.org/10.1016/S0261-3069(97)00062-9.
4. Nandan, R. DebRoy, T. and Bhadeshia, H.K.D.H. "Recent advances in friction-stir welding - Process, weldment structure and properties". *Prog. Mater. Sci.*, 53, pp. 980–1023 (2008). https://doi.org/10.1016/j.pmatsci.2008.05.001.
5. Sheikh, A.J.Y. Dima, S.A. Suleyman, D. et al. "Friction Stir Welding of High Density Polyethylene – Carbon Black Composite". *J. Mater. Process. Tech.*, 264, 402-413 (2019) https://doi.org/10.1016/j.jmatprotec.2018.09.033.
6. Liu, P. Li, Y. Geng, H. et al., J. "Microstructure characteristics in TIG welded joint of Mg/Al dissimilar materials". *Mater. Lett.*, vol. 61, pp. 1288–1291 (2007). https://doi.org/10.1016/j.matlet.2006.07.010.
7. Chi, C.T. Chao, C.G. Liu, T.F. et al. "Aluminum element effect for electron beam welding of similar and dissimilar magnesium-aluminum-zinc alloys". *Scr. Mater.*, vol. 56, pp. 733–736 (2007). https://doi.org/10.1016/j.scriptamat.2007.01.028
8. Thomas, W.M. Staines, D.G. Norris, I.M. et al. "Friction stir welding tools and developments". *Weld. World*, 47, pp. 10–17 (2003). https://doi.org/10.1007/BF03266403
9. Mishra, R. S. and Ma, Z. Y. "Friction stir welding and processing". *Mater. Sci. Eng. R Reports*, 50, pp. 1–78 (2005). https://doi.org/10.1016/j.mser.2005.07.001
10. Mehta, K. P. and Badheka, V. J. "Effects of Tilt Angle on Properties of Dissimilar Friction Stir Welding Copper to Aluminum". *Mater. Manuf. Process.*, 31(3) pp. 255-263 (2016). https://doi.org/10.1080/10426914.2014.994754

11. Sahu, S. Omkar, M., Surjya, K. P. et al., "Effect of weld parameters on joint quality in friction stir welding of Mg alloy to DP steel dissimilar materials", CIRP J. of Maf. Sci. and Tech., 35, pp. 502-516, (2021)
https://doi.org/10.1016/j.cirpj.2021.06.012.
12. Elyasi, M. Derazkola, H. A. and Hosseinzadeh, M. "Investigations of tool tilt angle on properties friction stir welding of A441 AISI to AA1100 aluminium. *J. Eng. Manuf.*, pp. 230(7):1234-1241 (2016).
https://doi.org/10.1177/0954405416645986
13. Muhayat, N. Zubaydi, A. Sulistijono, S. et al. "Effect of Tool Tilt Angle and Tool Plunge Depth on Mechanical Properties of Friction Stir Welded AA 5083 Joints", *Appl. Mech. Mater.*, 493, pp. 709–714 (2014).
https://doi.org/10.4028/www.scientific.net/AMM.493.709
14. Shah, P.H. and Badheka, V.J. "An Experimental Insight on the Selection of the Tool Tilt Angle for Friction Stir Welding of 7075 T651 Aluminum Alloys", *Indian J. Sci. Technol.*, 9, pp. 1–11 (2016).
DOI:10.17485/ijst/2016/v9iS1/102976
15. Meshram, S. D. and Reddy, G. M. "Influence of Tool Tilt Angle on Material Flow and Defect Generation in Friction Stir Welding of AA2219", *Def. Sci. J.*, 68, pp. 512–518 (2018).
DOI:10.14429/dsj.68.12027
16. Barlas, Z. "The Influence of Tool Tilt Angle on 1050 Aluminum Lap Joint in Friction Stir Welding Process", *ACTA Phys. Pol. A*, 132, pp. 679–681 (2017).
DOI: 10.12693/APhysPolA.132.679
17. Chitturi, V. Pedapati, S.R. and Awang, M. "Effect of Tilt Angle and Pin Depth on Dissimilar Friction Stir Lap Welded Joints of Aluminum and steel alloys", *Materials*, pp. 12(23)pp. 1-11 (2019).
https://doi.org/10.3390/ma12233901
18. Rajendran, C. Srinivasan, K. Balasubramanian, V. et al., "Effect of tool tilt angle on strength and microstructural characteristics of friction stir welded lap joints of AA2014-T6 aluminum alloy". *Trans. Nonferrous Met. Soc. China*, vol. 29, pp. 1824–1835 (2019).
https://doi.org/10.1016/S1003-6326(19)65090-9
19. Xia-wei, Y. Wu-yuan, F. Wen-ya, L. Xiu-rong, D. et al., "Microstructure and properties of probeless friction stir spot welding of AZ31 magnesium alloy joints", *Trans. of Nonfer. Met. Soc. of China*, 29(11)1, pp. 2300-2309, (2019)

https://doi.org/10.1016/S1003-6326(19)65136-8

20. Asadi, P. & Mirzaei, M.H. "Material flow modeling for the DSFSW of magnesium alloy", *The J. of Stn. Analysis for Engg. Desi.* 56(5):275-290 (2021) DOI:10.1177/0309324720976613
21. Mohammad, H.M. Parviz, A. Ali, F. "Effect of Tool Pin Profile on Material Flow in Double Shoulder Friction Stir Welding of AZ91 Magnesium Alloy", *Intl. J. of Mech. Sci,* 183, 105775, 0020-7403, (2020) https://doi.org/10.1016/j.ijmecsci.2020.105775
22. Cojocaru, R. Botila, L.N. & Dascau, H.F. "Friction Stir Welding in Inert Gas Environment (FSW-IG) of AZ31B Magnesium Alloy", *Deft and Diff. For*. 416. 21-29. (2022) https://doi.org/10.4028/p-cf745l
23. Ebenezer, D. KoteswaraRao, S.R. Harikrishna, K.L. et al., "Impression creep behavior of different zones in friction stir welded ZE41 magnesium-rare earth alloy", *Mat. Sci. and Engg: A*, 851, 143615, (2022) https://doi.org/10.1016/j.msea.2022.143615
24. AnilKumar, D. Waleed, A. Waleed, Z. et al., "Parametric Analysis on the Progression of Mechanical Properties on FSW of Aluminum-Copper Plates". *Adv. in Sci. and Tech. Res. J.*, 16(2), 168–178(2022) https://doi.org/10.12913/22998624/147123
25. Tianhao, W. Shivakant, S. Bharat, G. et al., "Effect of reactive alloy elements on friction stir welded butt joints of metallurgically immiscible magnesium alloys and steel", *J. of Manuf. Proc.*, 39, pp. 138-145, (2019) https://doi.org/10.1016/j.jmapro.2019.02.009
26. Chunliang, Y. ChuanSong, W. Lei, S. "Modeling the dissimilar material flow and mixing in friction stir welding of aluminum to magnesium alloys", *J. of Alloys and Comp.* 843, 156021, (2020) https://doi.org/10.1016/j.jallcom.2020.156021
27. Singh, Umesh & Dubey, Avanish. "Microstructure, mechanical and corrosion behaviours in friction stir welding of dissimilar magnesium alloys", Mater. and Corr., 74, 1217–1232 (2023) https://doi.org/10.1002/maco.202313798
28. Liangwen, X. Xianyong, Z. Weijia, S. et al., "Investigations on the material flow and the influence of the resulting texture on the tensile properties of dissimilar friction stir welded ZK60/Mg–Al–Sn–Zn joints", *J. of Mat. Res. and Tech.* 17, pp. 1716-1730,(2022)

DOI:10.1016/j.jmrt.2022.01.127

29. Goyal, A. and Garg, R. "Modeling and optimization of friction stir welding parameters in joining 5086 H32 aluminium alloy". *Scientia Iranica*, *26*(4), 2407-2417. (2019) DOI: 10.24200/SCI.2018.5525.1325
30. Delir, N.R. Nemati, A.B. Omidbakhsh, F. "Optimization of friction stir welding parameters with Taguchi method for maximum electrical conductivity in Al-1080 welded sections". *Scientia Iranica, 28*(4), 2250-2258. (2021) DOI: 10.24200/SCI.2021.56528.4772
31. Prabhu, S. Shettigar, A. Herbert, M.A. et al., "Optimization of FSW process parameters for maximum UTS of AA6061/rutile composites using Taguchi technique". *Scientia Iranica*, *29*(2), 534-542. (2022) DOI: 10.24200/sci.2021.56624.4816
32. Ankit, T. Varun, S. Shailendra, S. "Effect of tool tilt angle on weld joint strength and microstructural characterization of double-sided friction stir welding of AZ31B magnesium alloy", *CIRP J. of Manuf. Sci. and Tech.* 35, Pages 132-145, (2021) https://doi.org/10.1016/j.cirpj.2021.05.009.
33. Liangwen Xie, Xianyong Zhu, Yuexiang Fan, Song Yang, Cheng Jiang, Yulai Song, Evolution and distribution of crystallographic texture on friction-stir welded joint of Mg-4.6Al-1.2Sn-0.7Zn magnesium alloy, Journal of Materials Research and Technology, Volume 20, Pages 3836-3842, (2022), ISSN 2238-7854, https://doi.org/10.1016/j.jmrt.2022.08.146.
34. Liangwen, X. Xiong, X. Xianyong, Z. et al., "Influence mechanism of pin thread in friction stir welding of magnesium alloys based on the relationship between microstructure and mechanical properties", *J. of Mat. Pro. Tech*., 312, (2023) https://doi.org/10.1016/j.jmatprotec.2023.117870
35. Fernanda, R.C. Bruna, F.B. Luciano, A.B. et al., "Effect of the gap width in AZ31 magnesium alloy joints obtained by friction stir welding", J. of Mat. Res. and Tech. 15, pp. 5297-5306, (2021) DOI:10.1016/j.jmrt.2021.10.115
36. Zhe, L. Zhiyu, F. Li, L. et al., "Refill friction stir spot welding of AZ31 magnesium alloy sheets: metallurgical features, microstructure, texture and mechanical properties", *J. of Mater. Res. and Tech.* 23, pp. 3337-3350, (2023) https://doi.org/10.1016/j.jmrt.2023.01.151
37. Unnikrishnan, M.A. EdwinRaja, D.J. Anton, S.L.K. et al., "Challenges on friction stir

welding of magnesium alloys in automotives", *Mat. Today: Proceedings*, (2023), ISSN 2214-7853, https://doi.org/10.1016/j.matpr.2023.03.789

38. Mostafa, A., Parviz, A. Hossein, R. et al., "Investigation of wear and microstructural properties of A356/ Tic composites fabricated by FSP". *Surf. Rev. and Lett*. 29(10) pp.1-10 (2022) https://doi.org/10.1142/S0218625X2250130X
39. Zheng, F.Y. Wu, Y. Peng, L. et al., "Microstructures and mechanical properties of friction stir processed Mg–2.0Nd–0.3Zn–1.0Zr magnesium alloy". J. of Mag. and All.. 1. pp.122–(2013) https://doi.org/10.1016/j.jma.2013.06.001
40. Salami, P. Khandani, T. Asadi, P. et al., "Friction stir welding/processing as a repair welding." *Advances in Friction-Stir Welding and Processing* 10 (2014) https://doi.org/10.1533/9780857094551.427
41. Gollo, R. Sandeep, S. Yadaiah, N. et al., "Experimental investigation of defect formation, microstructure and mechanical properties in friction stir welding of AA5086". *Metall. Res. Technol*. 119, 514 (2022) https://doi.org/10.1051/metal/2022068
42. Abdullah, M.E. Rohim M.N. Mohammed, M.M. et al., "Effects of Partial-Contact Tool Tilt Angle on Friction Stir Welded AA1050 Aluminum Joint Properties". *Materials*. 16(11):4091 (2023) https://doi.org/10.3390/ma16114091

Biography:

Dr. Anil Kumar Deepati is currently working as an Assistant Professor and Coordinator of the Department of Mechanical Engineering Technology, College of Applied Industrial Technology, Jazan University, Kingdom of Saudi Arabia. He received his Ph.D. in Mechanical Engineering from the Indian Institute of Technology Guwahati, India in 2015. He received his First Degree in Mechanical Engineering and Master's in Mechanical Engineering specializing in Advanced Manufacturing systems from Jawaharlal Nehru Technological University Hyderabad, India. His areas of research interest are Advanced Welding technologies, Friction Stir welding, Composite materials, Materials characterization, NDT, etc.

Figure Captions:

Figure 1. The basic principle of FSW and the parts of FSW tool

Figure 2. Various FSW joint types (i, ii) Square butt and lap joint, (iii) Edge joint, (iv, v) Square and butt T-joint, and (vi) Fillet joint.

Figure 3. Schematic illustration of FSW parameters.

Figure. 4. Photograph of friction stir welding setup.

Figure. 5 The dimensions of the tensile test specimen in millimetres according to the ASTM E8 norms.

Figure. 6**.** Photograph of FSW joints achieved at different tool tilt angles: (c) 0^o, (d) 1^o, (b) $2^{o,}$ and (a) 3^o.

Figure. 7. Macrographs of the transverse section of joints produced under different tool tilt angles: (A) 0^o, (B) 1^o, (C) $2^{o,}$ and (D) 3^o

Figure. 8. Microstructure of base metal wrought magnesium alloy.

Figure. 9. Microstructure detail of (a) HAZ and (b) TMAZ

Figure 10. Weld nugget zone microstructure of the welds created with various tilt angles: (a) 0^o, (b) 1^o, (c) $2^{o,}$ and (d) 3^o.

Figure 11. Hardness profile of the FSW joints made with various tilt angles.

Figure 12 A Photograph of tensile specimens before and after the fracture.

Figure 13. Tensile properties of the joint made with various TA's.

Table Captions:

Table 1 Lists the chemical composition of wrought magnesium alloy (in weight %).

Table 2 Lists the wrought magnesium alloy's mechanical characteristics.

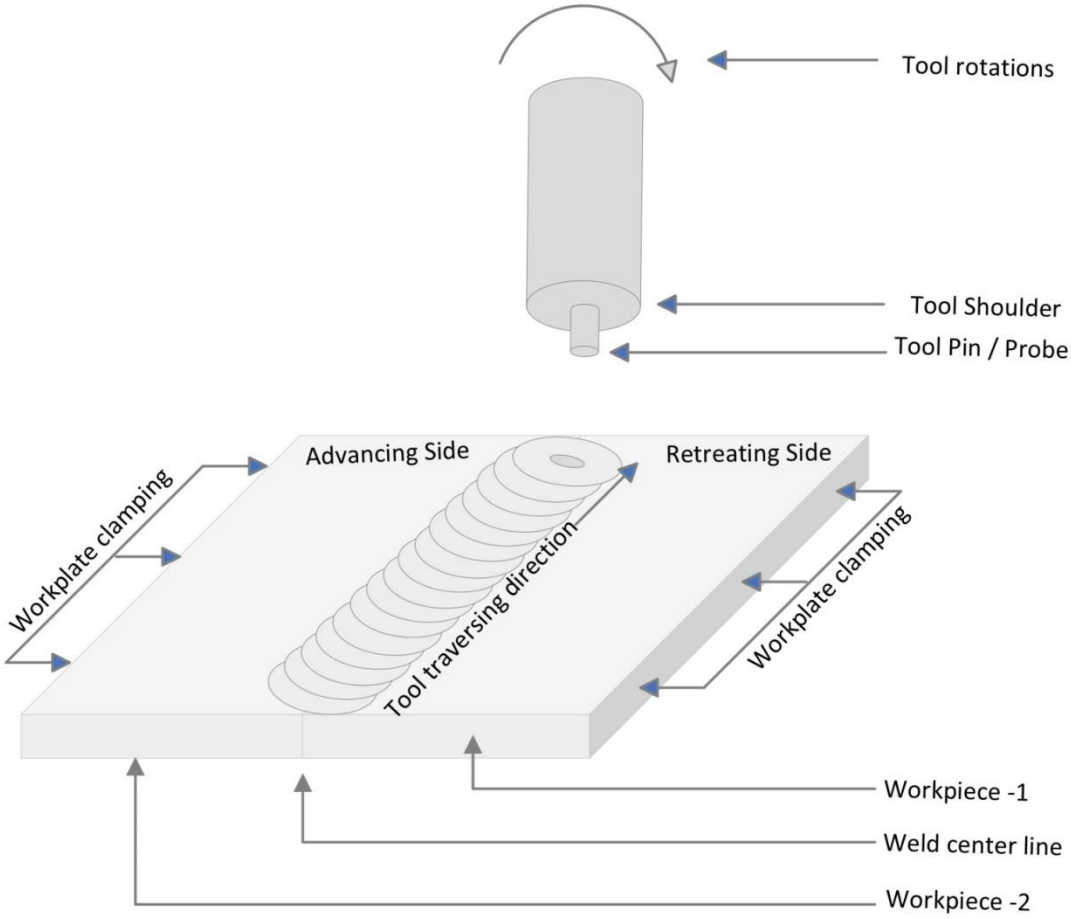

Figure 1. The basic principle of FSW and the parts of FSW tool

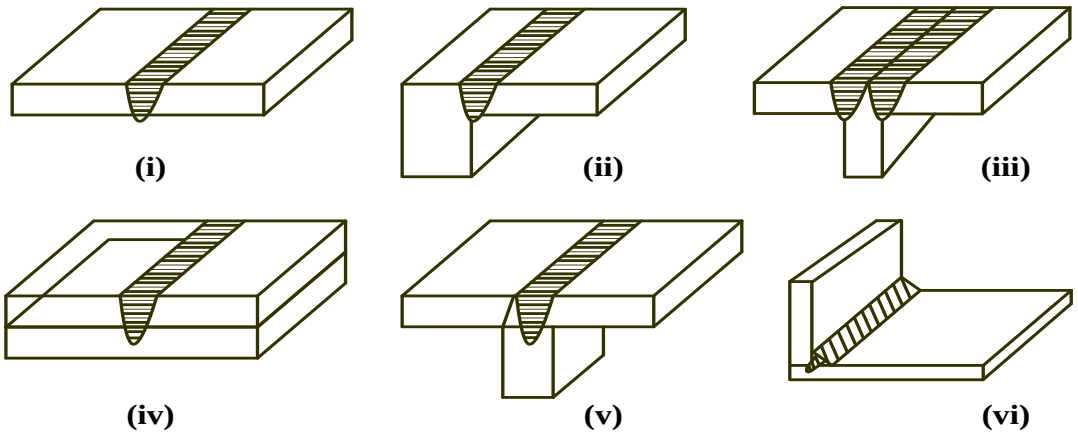

Figure 2. Various FSW joint types (i, ii) Square butt and lap joint, (iii) Edge joint, (iv, v) Square and butt T-joint, and (vi) Fillet joint.

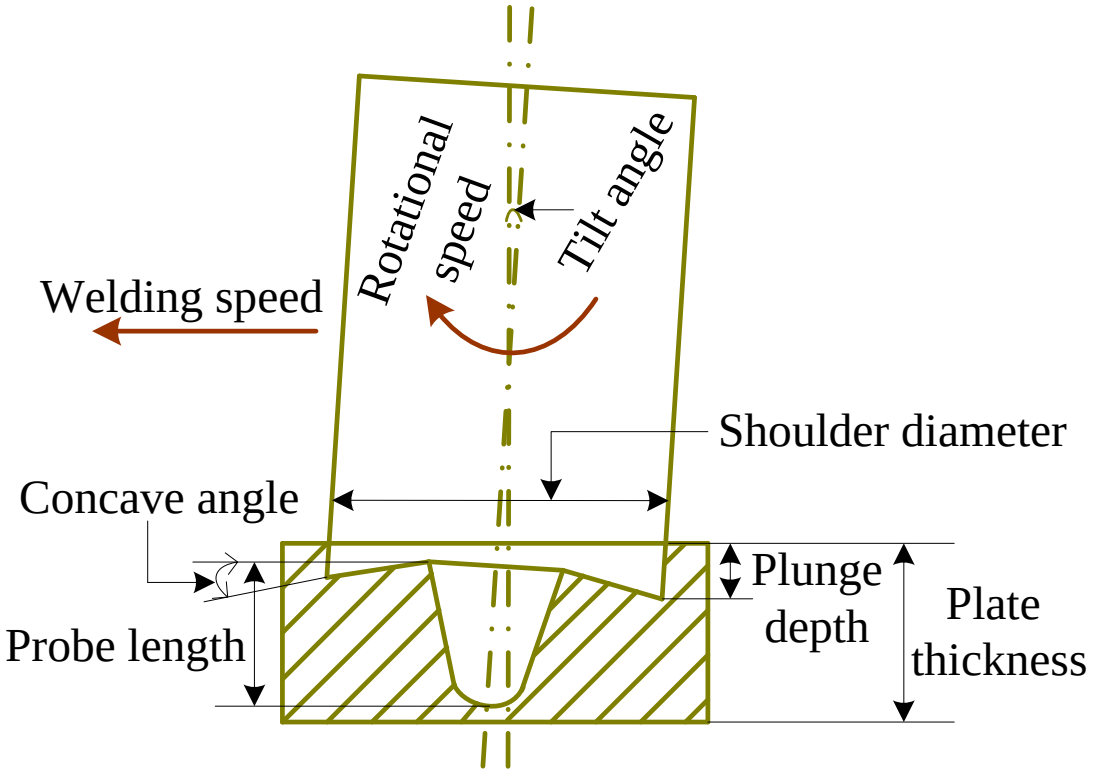

Figure 3. Schematic illustration of FSW parameters.

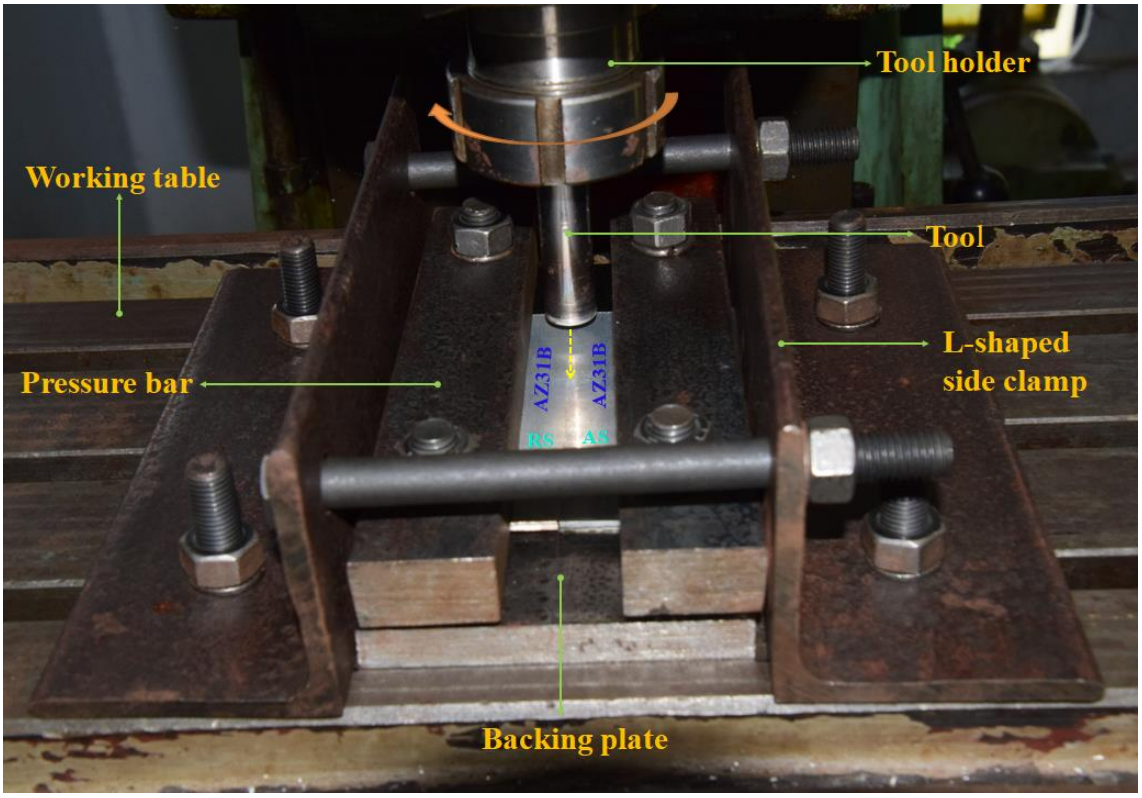

Figure. 4. Photograph of friction stir welding setup.

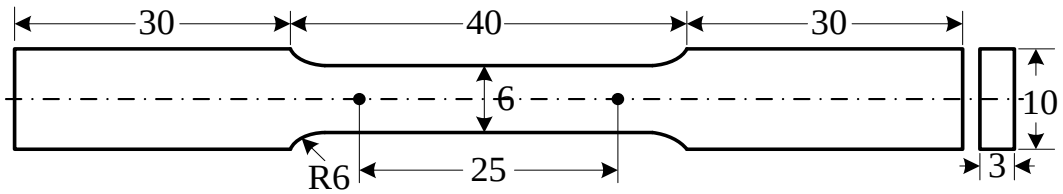

Figure. 5 The dimensions of the tensile test specimen in millimeters according to the ASTM E8 norms.

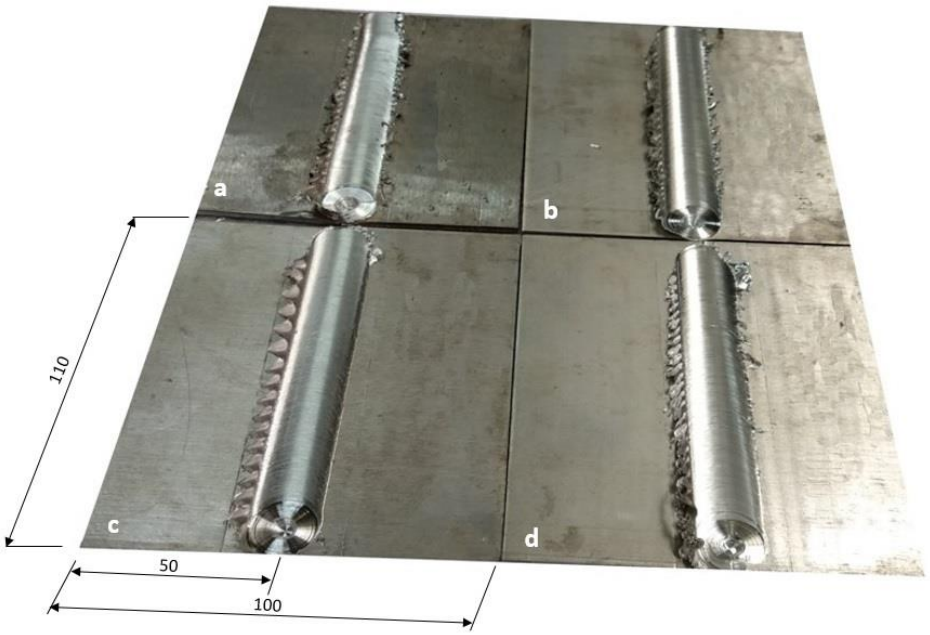

Figure. 6. Photograph of FSW joints achieved at different tool tilt angles: (c) 0^{o}, (d) 1^{o}, (b) $2^{o,}$ and (a) 3^{o}.

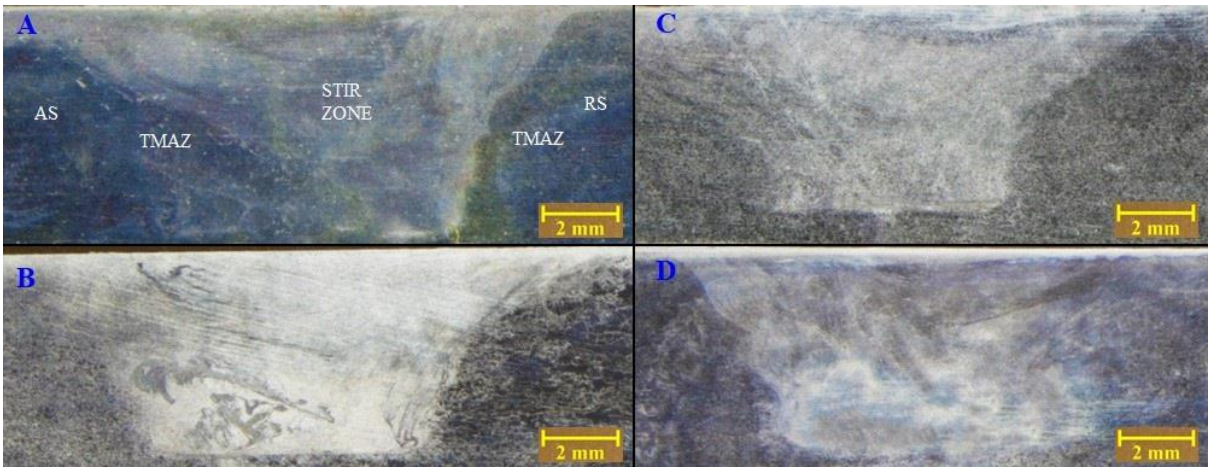

Figure. 7. Macrographs of the transverse section of joints produced under different tool tilt angles: (A) 0^{o}, (B) 1^{o}, (C) $2^{o,}$ and (D) 3^{o}

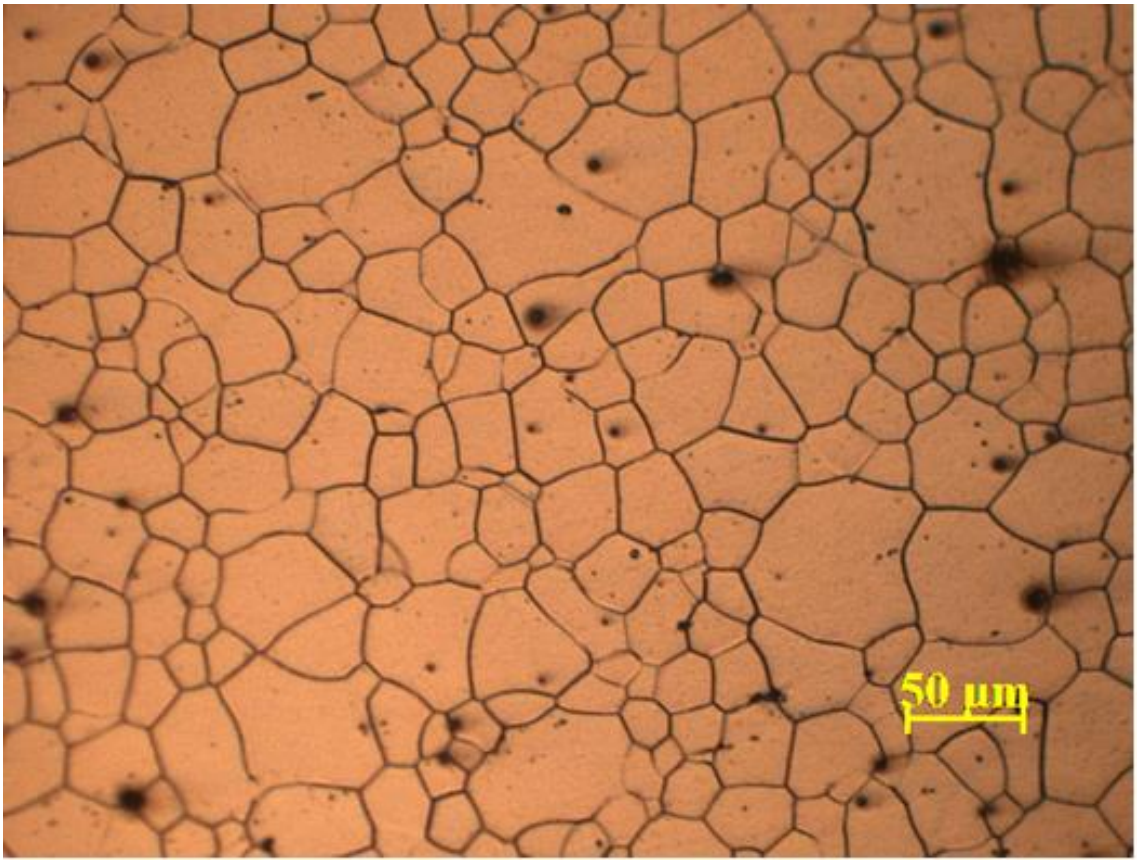

Figure. 8. Microstructure of base metal wrought magnesium alloy.

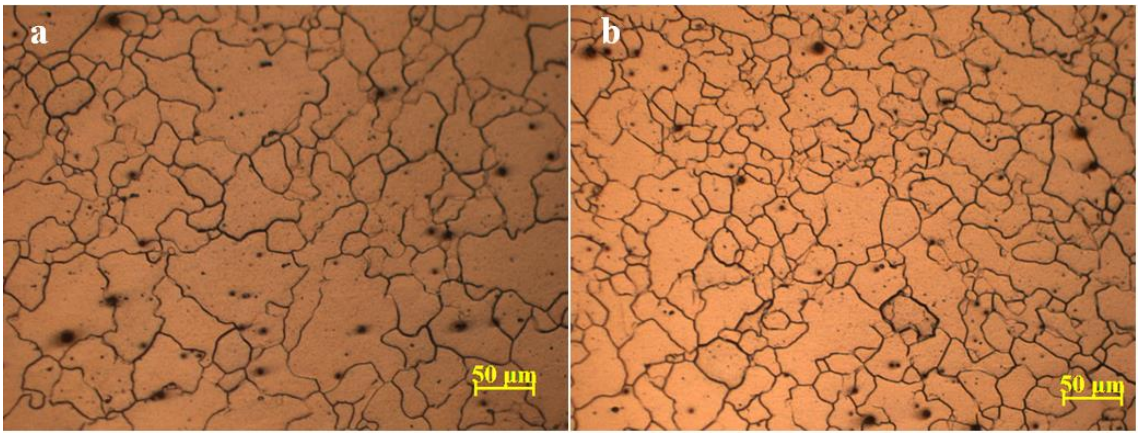

Figure. 9. Microstructure detail of (a) HAZ and (b) TMAZ

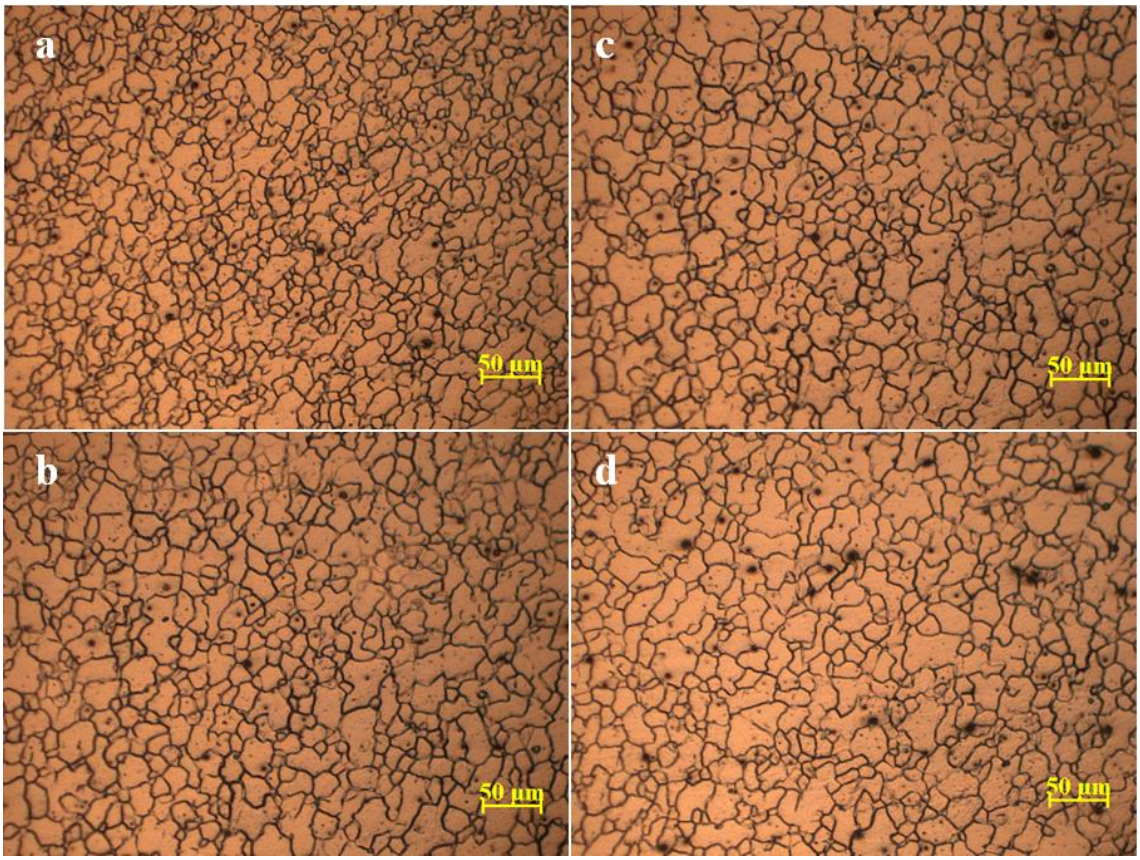

Figure 10. Weld nugget zone microstructure of the welds created with various tilt angles: (a) 0^{o}, (b) 1^{o}, (c) $2^{o,}$ and (d) 3^{o}.

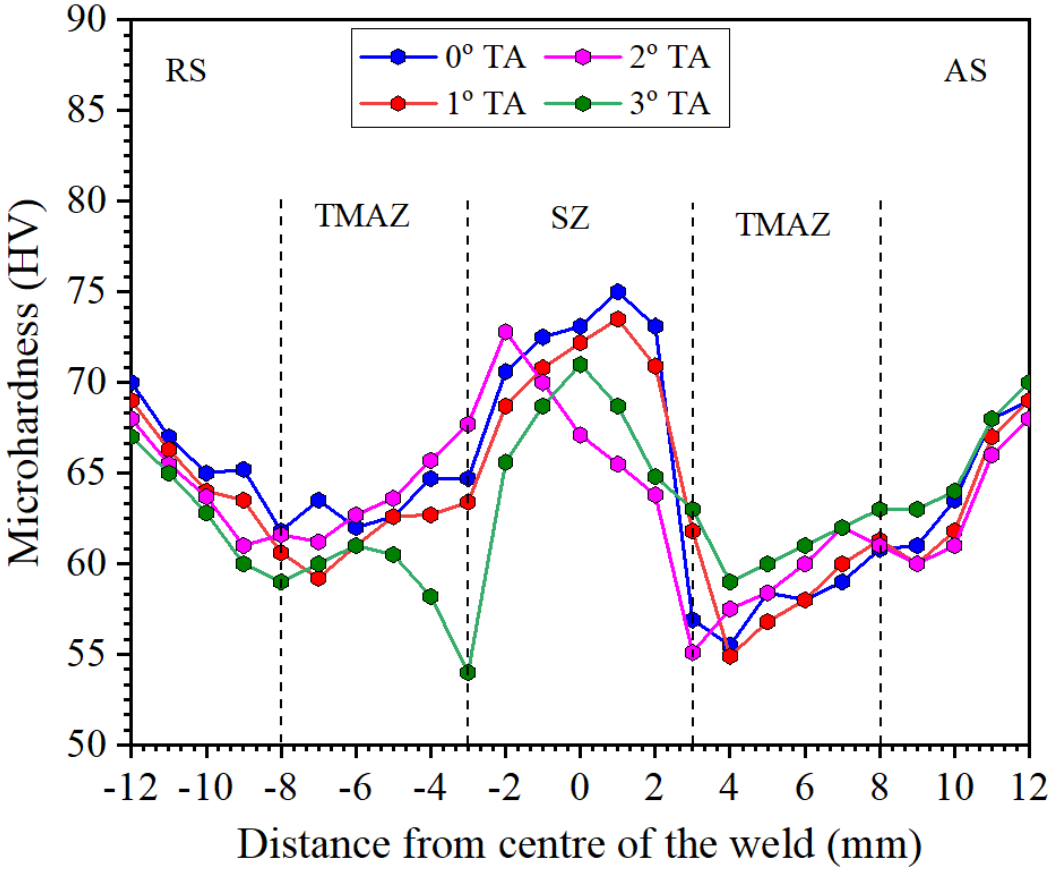

Figure 11. Hardness profile of the FSW joints made with various tilt angles.

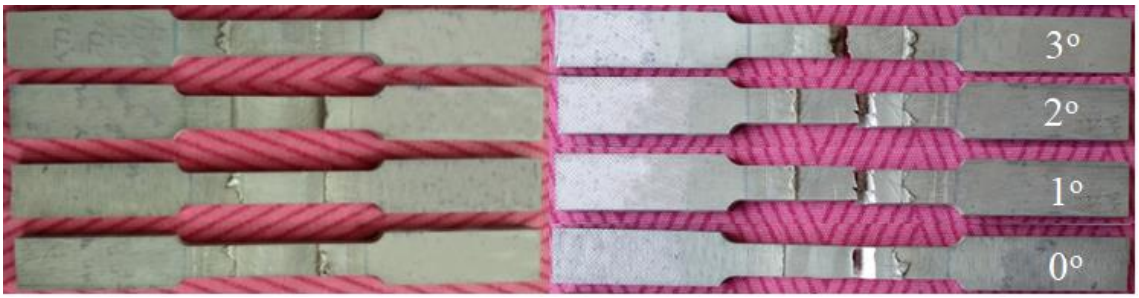

Figure 12**.** A Photograph of tensile specimens before and after the fracture.

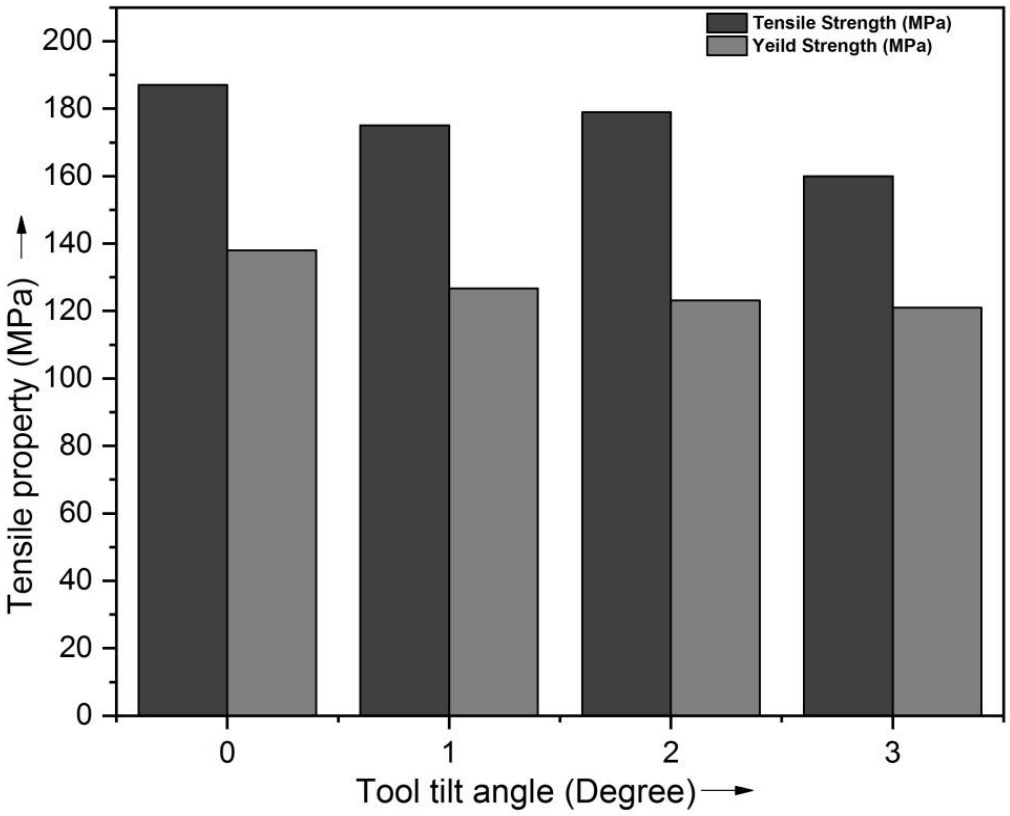

Figure 13. Tensile properties of the joint made with various TA's.

Table 1. Lists the chemical composition of wrought magnesium alloy (in weight %).

Material	Si	M	Fe	Ca	Cu	Ni	Ti	Al	Zn	Mg
AZ31B	0.005	0.29	0.002	0.03	0.001	0.002	0.021	2.79	0.79	96.07

Table 2. Lists the wrought magnesium alloy's mechanical characteristics.

UTS (MPa)	YS (MPa)	Elongation Ɛ (%)	Hardness (HV)
247	154	17	71